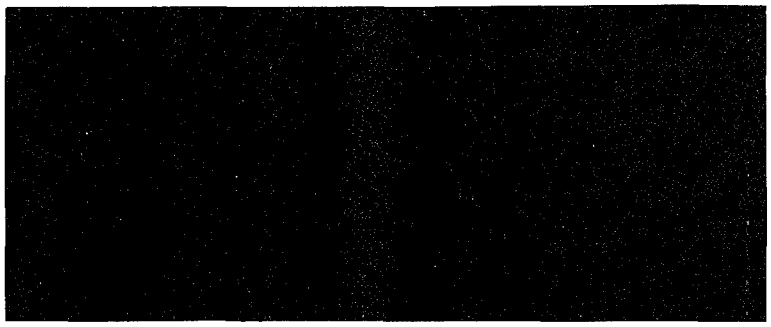

The Jamie Whitten National Center for Physical Acoustics

The University of Mississippi

FINAL TECHNICAL REPORT

FOR

OFFICE OF NAVAL RESEARCH

CONTRACT N00014-94-1-0974

ENTITLED

NCPA RESEARCH PROGRAM, FY94

OCTOBER 1995

NCPA Internal Tracking Number: LC1095-2

National Center for Physical Acoustics
University of Mississippi and
Mississippi Resource Development Corporation

REPORT DOCUMENTATION PAGE

Form Approved
OMB No. 0704-0188

1. AGENCY USE ONLY *(Leave blank)*	2. REPORT DATE	3. REPORT TYPE AND DATES COVERED
	31 OCT 95	Final Technical; 1 Jun 94 to 31 May 95

4. TITLE AND SUBTITLE

Final Technical Report; NCPA Research Program, FY94

5. FUNDING NUMBERS

PE 61153N
G N00014-94-1-0974
TA 0044337 & 0044374

6. AUTHOR(S)

H.E. Bass, A.R. Kolaini, B. Denardo, and J.M. Sabatier

7. PERFORMING ORGANIZATION NAME(S) AND ADDRESS(ES)

University of Mississippi
Jamie Whitten National Center for Physical Acoustics
University, MS 37677

8. PERFORMING ORGANIZATION REPORT NUMBER

LC1095-2

9. SPONSORING/MONITORING AGENCY NAME(S) AND ADDRESS(ES)

Office of Naval Research Detachment
Code 322
1020 Blach Blvd.
Stennis Space Center, MS 39529-5004

10. SPONSORING/MONITORING AGENCY REPORT NUMBER

11. SUPPLEMENTARY NOTES

12a. DISTRIBUTION/AVAILABILITY STATEMENT

Approved for public release; distribution unlimited.

12b. DISTRIBUTION CODE

13. ABSTRACT *(Maximum 200 words)*

This report summarizes research performed at the Jamie Whitten National Center for Physical Acoustics during the period June 1, 1994 to May 31, 1995. Research on bubble related ambient noise in the ocean is a continuation of a long term research project into this phenomenon. Experimental investigation of an acoustic soliton is a new effort. The research into attenuation mechanisms in sediments attempts to apply past research expertise in propagation through air filled soils to the underwater case. The long term research project into active surfaces was discontinued. The NCPA Graduate Fellowship program continues to provide a supply of very well qualified Ph.D. graduates. The new initiative in the physics of acoustics is the imaging of buried objects.

14. SUBJECT TERMS

Bubble related ambient noise; acoustic soliton; attenuation mechanisms; active surfaces; acoustic imaging

15. NUMBER OF PAGES

36

16. PRICE CODE

17. SECURITY CLASSIFICATION OF REPORT	18. SECURITY CLASSIFICATION OF THIS PAGE	19. SECURITY CLASSIFICATION OF ABSTRACT	20. LIMITATION OF ABSTRACT
UNCLASSIFIED	UNCLASSIFIED	UNCLASSIFIED	

TABLE OF CONTENTS

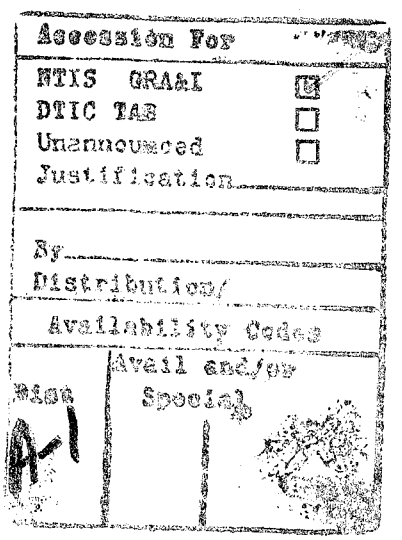

INTRODUCTION

This report summarizes research performed at the Jamie Whitten National Center for Physical Acoustics during the period June 1, 1994 to May 31, 1995. Research on bubble related ambient noise in the ocean is a continuation of a long term research project into this phenomenon. Research this year has been concerned, primarily, with collective behavior of bubble clouds. Experimental investigation of an acoustic soliton is a new effort. The major thrust of this research program is to explore new discoveries in nonlinear phenomena. The research into attenuation mechanisms in sediments attempts to apply past research expertise in propagation through air filled soils to the underwater case. This year, the long term research project into active surfaces, specifically an active rigid wall impedance tube was discontinued. This project has progressed to the point where specific applications are in order and are being pursued with a different sponsor. The NCPA Graduate Fellowship program continues to provide a supply of very well qualified Ph.D. graduates. The new initiative in the physics of acoustics is the imaging of buried objects. This rather applied project is scheduled to last only two years.

The research projects listed above and described in this report span the range from very basic to very applied. It is the goal of NCPA to allow worthwhile research projects to follow this developmental path. Success of this approach is heavily dependent upon feedback from the user community. Your comments and suggestions are always appreciated.

BUBBLE RELATED AMBIENT NOISE IN THE OCEAN

ABSTRACT

This is an experimental study addressing the role of the individual bubbles and bubble clouds which give rise to the ambient noise in the ocean. These bubble clouds are produced by breaking waves in a controlled and repeatable laboratory anechoic tank/wavemaking facility. The mechanical properties of the bubble clouds generated by various 2–D and 3–D breakers, in fresh and salt water, and their acoustical properties (both passive and active) were investigated. Sound production mechanisms in a turbulent flow containing bubbles were also investigated.

SUBTASK I – BUBBLE–RELATED NOISE FROM BREAKING WAVES

Over the years considerable attention has been devoted to the understanding of ambient sound in the ocean. Breaking waves are now believed to be the main source of wind–generated ambient noise. Recent conferences devoted to the understanding of the source mechanisms for ambient noise production at the sea surface have lent further support to the contributions of gas bubbles as the principal source of this noise.[1–3] However, a detailed description of the specific role of bubbles has not yet been given. The accurate determination of the source level from wind–generated ambient noise ultimately relies on our understanding of the physics of wave breaking and sound generation mechanisms which are presently being actively investigated. Bubbles created by breaking waves at sea are recognized to be the major factor in the Knudsen[4] wind noise generation, radar backscattering, and sea surface acoustic reverberation. Breaking waves give rise to bubble plumes which penetrate a distance of several meters under the ocean surface and persist for as long as several minutes. These clouds play an important role in the reverberation and backscattering of underwater sound of immediate and high sea states. In the last decade, there has been quite a number of studies conducted in laboratories and fields that have shed some light on the complex nature of ambient noise generation by breaking waves. The results of laboratory studies have shown that the sources of noise are newly created bubbles oscillating at their linear resonance frequency and collective oscillations of bubble clouds.[5–7] The sound generated by breaking waves at sea has been used to measure their spatial and temporal properties.[8] Recent open ocean measurements of the noise generated by breaking waves[9–10] and the free field and laboratory measurements of the noise generated by transient water jets[11–13] in fresh and salt water suggest that the sound pressure spectra and levels depend upon the salinity of the water and the frequency of the noise could range as low as several tens of Hz. In addition to the numerous experimental studies, there have been several recent theoretical analyses of noise generation by breaking waves,

where these would typically predict on the general behavior of the noise levels in terms of slopes and order of magnitude estimates.[14–15]

The acoustic backscattering phenomena from bubble clouds generated by breaking waves are not yet fully understood. A significant discrepancy exists between the observed scattering of sound from the sea surface and the values predicted by the classic theory of Bragg scattering from rough surfaces at wind speeds in excess of 10 m/s. The recent advances in surface scattering theory provide reasonable assessments of the backscattering strength from rough surfaces. With these new developments, there still remains a 15 to 20 dB discrepancy between surface scattering calculations and measured reverberation levels[16–17] at high sea states. It is unlikely that the discrepancy can be removed by further improving the rough surface scattering theory. Recent published works indicate a significant role for bubble clouds in surface backscatter.

The principal focus of this task is to investigate both theoretically and experimentally the hydrodynamics and acoustic characteristics of bubble clouds generated by laboratory breaking waves in fresh and salt water.

RESEARCH PROGRESS IN FY94

(A) Experimental Observations

The measurements of the absolute sound pressure levels obtained for various breaker intensities in fresh water are reported in an article that appeared in JASA.[18] The detailed description of the experimental setup, data collection, and data analysis are also reported in this paper. Figure 1 shows a typical photograph of a moderate spilling breaker produced in a laboratory tank. In fresh water, we have observed a gradual transition from relatively low intensity, high frequency acoustic emissions from gently spilling breakers to relatively high intensity, low frequency emissions from plunging breakers. For the gentle spilling breakers, small numbers of individual bubbles of small size were produced. It appeared as if the majority of sound was produced by these individual bubbles resonating at their natural frequencies. However, as the intensity of the breaker was increased, more bubbles were produced. Although the size of the bubbles became larger, they did not become large enough for the individual bubbles radiating alone to account for the full range of acoustic emissions observed. We interpret this behavior to result from the fact that individual bubbles were experiencing the influence of their nearest neighbors, and thus radiated at a lower frequency because of mass loading. As the breaking waves approached more toward a plunging breaker, the concentration of bubbles and the associated void fraction became larger, the dynamics of the breaking process lead to the production of eddies, and the acoustic emissions extended to the very low frequencies (< 200 Hz). It appeared that, in this case, compact bubble clouds were radiating as a unit, in the form of collective oscillations.

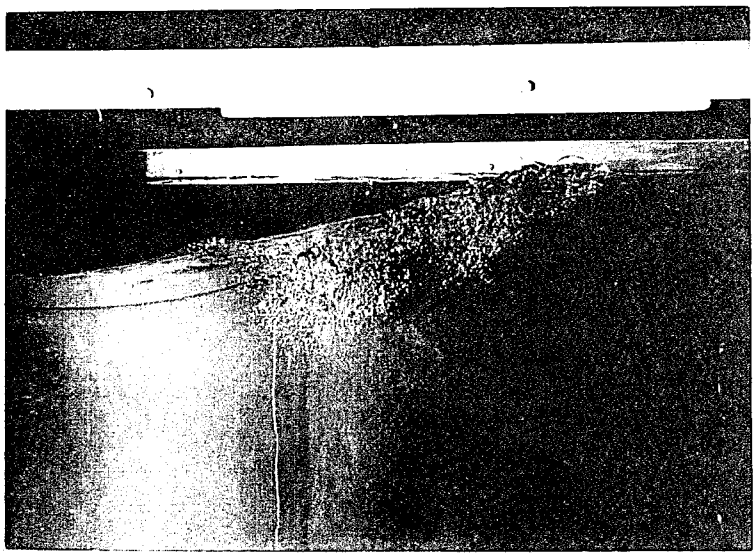

Figure 1. A typical photograph of a moderate spilling breaker produced in freshwater.

The results reported in FY 93 were produced in fresh water, which tends to entrain larger bubbles than similar–sized breakers produced in salt water. Accordingly, we have extended our laboratory results to the salt water case. The salinity of water in the tank was increased to 33/1000. Figures 2–3 show power density plots for weak and moderate spilling breakers, respectively. The power densities in these figures were averaged over 100 samples and are compared with those measured in fresh water. The power densities shown in Figs. 2a–b for weak spilling breakers in fresh and salt water, respectively, have a prominent broad peak around 2–3 kHz. The spectral slope of the noise from the weak breaker is roughly 6 dB/octave from 2 kHz to 20 kHz and follows f^{-2} and remains the same for these two water mediums. The power density of moderate breakers also indicates a shift to lower frequencies in salt water. The spectral slope is roughly 5 dB/octave from 500 Hz to 25 kHz and is the same as fresh water (Figs. 3a–b). The spectral slopes resemble the Knudsen wind wave spectra at sea with 5–6 dB/octave fall–off in the frequency range 0.5–25 kHz. As the intensity of a breaking wave increases or in the open ocean case, as the wind speed increases, there is an associated increase in the magnitude of the acoustic radiation and a gradual shift to lower frequencies.

The striking difference between salt and fresh water is the increase in sound pressure level in salt water compared to fresh water. This difference is expected for the reason that more bubbles are produced per breaking wave in salt water than in fresh. Most bubbles that are produced radiate at their natural or resonance frequencies; thus, the number of sources would be more important than the sizes of the bubbles (i.e., more smaller bubbles would be more important than less larger bubbles). We are in the process of measuring the histogram of the bubble size distribution in salt water. Another very important observation is shown in the weak spectra (Figs. 2a–b), where in salty medium, because of an increase in the number of smaller bubbles in salt water, the individual

bubbles are experiencing the influence of their nearest neighbors, and thus radiate at a lower frequency. The 3–4 dB increase in sound pressure level in the frequency range 100–400 Hz (Fig. 2b) clearly shows this effect. We begin to see collective oscillations of the bubble cloud generated by a weak spilling breaker in salt water and the absence of these oscillations in fresh water for the same breaker.

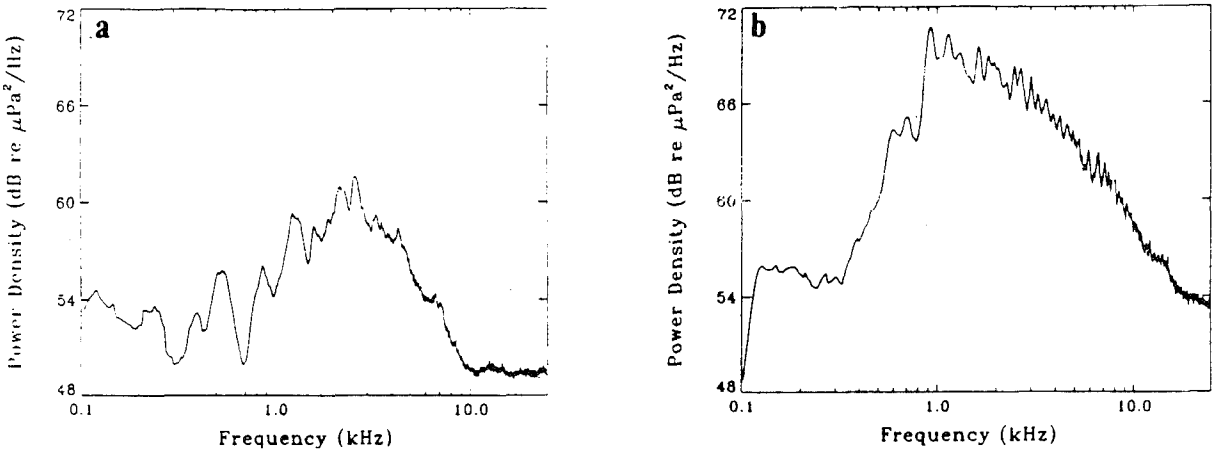

Figure 2. Power densities averaged over 100 acoustic signals generated by weak spilling breakers. (a) Fresh water and (b) Salt water.

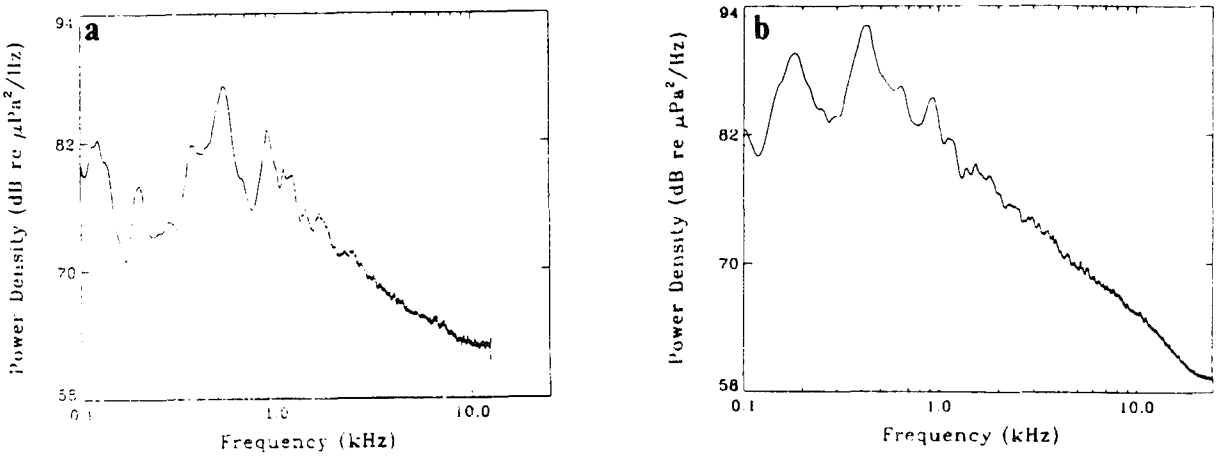

Figure 3. Power densities averaged over 100 acoustic signals generated by moderate spilling breakers. (a) Fresh water and (b) Salt water.

In modeling the sound pressure level of bubble clouds generated by laboratory breaking waves, besides the bubble size distribution and void fraction measurements, the nature of the sources of sound and cloud dimensions as a function of time from breaker onset are important parameters to measure. Figure 4 shows the non–dimensional acoustic pressure of moderate spilling breakers as a function of angle from the water surface. This figure shows the dipole behavior of the sound generated by breaking waves. Figure 5 shows the breaker cross–sectional area (bubble cloud cross–section) for a typical spilling breaker as a function of time. The bubble

cloud generated by the breaker grows approximately linearly from the onset of the breaker, reaching a maximum at about one second, which is close to the period of acoustic emission, and then declines due to loss of breaker heights. In the growth region bubbles of various sizes were generated. Once the bubble cloud cross–section reaches its maximum, the air entrainment ceases. During the bubble cloud growth, it consists of primarily large bubbles with a large amount of air (average void fraction 10%). After reaching its maximum growth, larger bubbles tend to move to the surface due to the buoyancy force. The air–content in the declining region of the cloud, which consists of smaller bubbles, decreased and remained in the water for a longer period (average void fraction ~0.3%).

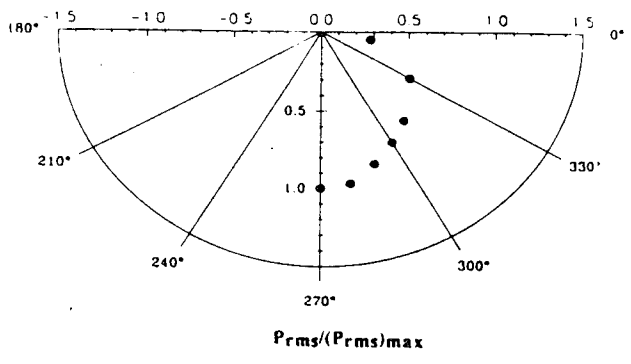

Figure 4. The RMS sound pressure distribution as a function of angle for moderate spilling breakers. The dipole behavior of the sound generation by breaking waves are evident.

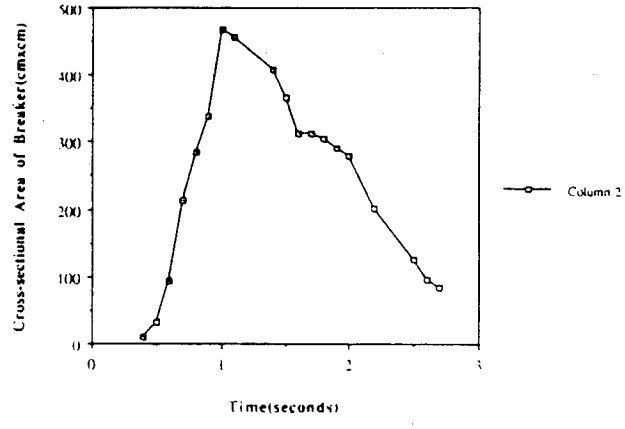

Figure 5. The growth and collapse of the cross-sectional area of bubble clouds generated by a moderate spilling breakers.

The backscattering properties of the bubble cloud generated by moderate spilling breakers are investigated for frequencies ranging from 15–40 kHz. Figure 6 shows the experimental setup for this purpose. Wave generation and data accumulation was fully automated using the LabView 3.0.1 software system.[19] The active measurements was conducted by sending a burst of sound into a bubble cloud produced by spilling breakers at the instant the void fraction of the bubble cloud was reduced from a maximum of 10% to around 0.3% when the passive noise from it had subsided. The scattering strength from rough surfaces were isolated by generating two different sets of gravity waves. The first set of gravity waves were generated with enough energy to break at the middle section of the tank, creating a bubble cloud just beneath the water surface. The second set possessed the same frequency band as the set that produced moderate spilling breakers, but lacked the energy to break. Figure 7 shows the results of the scattering strength measurements from breaking waves at a grazing angle of 45° as a function of frequency and vertical angle. Scattering strengths tend to decrease with an increase in incident frequency and levels remain about

Backscattering schematic:

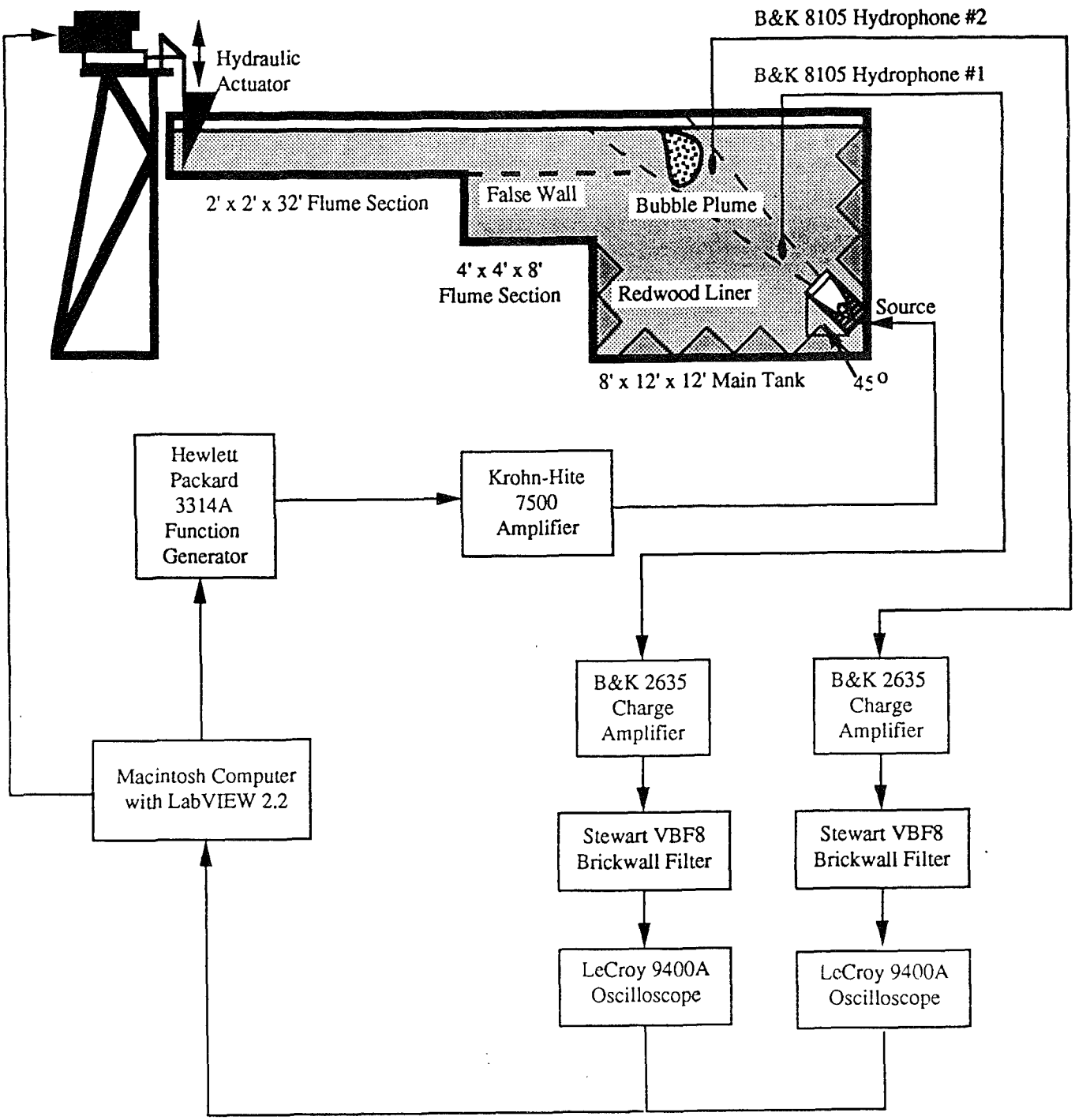

Figure 6. Schematic drawing of the experimental apparatus used to study the backscattering of sound from breaking waves.

the same with an increase in the vertical angle. The scattering strengths from rough surfaces without bubble clouds also decrease with frequency, but seemed to increase slightly with an increase in the vertical angle. The slight increase in the backscattering levels from rough surfaces may be due to capillary ripples that existed on the front face of the gravity waves when the sound was incident upon it.

The backscattering measurement as a function of frequency is shown in Fig. 8 at a grazing angle of 45° and along the incident beam. The pronounced peaks at around 20 and 30 kHz, along with the histogram of the bubble size distribution at the instant when incident waves strike the bubble cloud (Fig. 9), show that the bubble resonance may play a big role in these observations.

(B) Theoretical Considerations

We have undertaken the task to model the experimental observations of the acoustical characteristics from various types of breaker intensities. Observations in both fresh and salt water indicate that sound radiation by gentle spilling breaking waves is due mostly to single bubble oscillations. For the case of stronger breakers, it appears that both individual bubble oscillations and collective bubble cloud oscillations contribute to the spectra, especially at lower frequencies. Calculations of sound spectra using individual damped oscillations corroborate these gentle spill measurements where models for an array of dipole sources for each bubble size is used with frequency–dependent attenuation in the thermal damping regime.[20] Work is continuing on predicting the collective bubble oscillation contribution to the noise spectrum for the more severe breakers. We expect to use the computer model developed by Oguz[15] with modification for adaptation to this problem. Most recent backscattering models include a low frequency scattering from clouds away from bubble resonance where sound speed is drastically reduced to as low as a few tens of meters per second.

Only recently the resonance of bubbles has been included in the backscattering model.[21] Bubble clouds generated in the laboratory tank contain larger bubbles whose resonance frequencies are in the range of the incident frequencies. In this case, the sound speed in the cloud could be faster than in pure water. We have begun developing a backscattering model that will incorporate a semi–cylindrical bubble cloud situated near the free surface. We assume the semi–cylinder is sufficiently long to ignore the end effects, the bubble cloud is homogeneous in space, and bubble size distribution will be identified from measurements (see Fig. 9). The governing equation for the incident waves striking the cloud at a right angle with the axis of the semi–cylinder is the Helmholtz equation in and outside the cloud. The general solution in the cloud and outside the cloud can be obtained by solving the Helmholtz equation by applying the boundary conditions at the interface and the pressure release condition at the air–water interface. The sound speed in the bubbly liquid will have a form of,

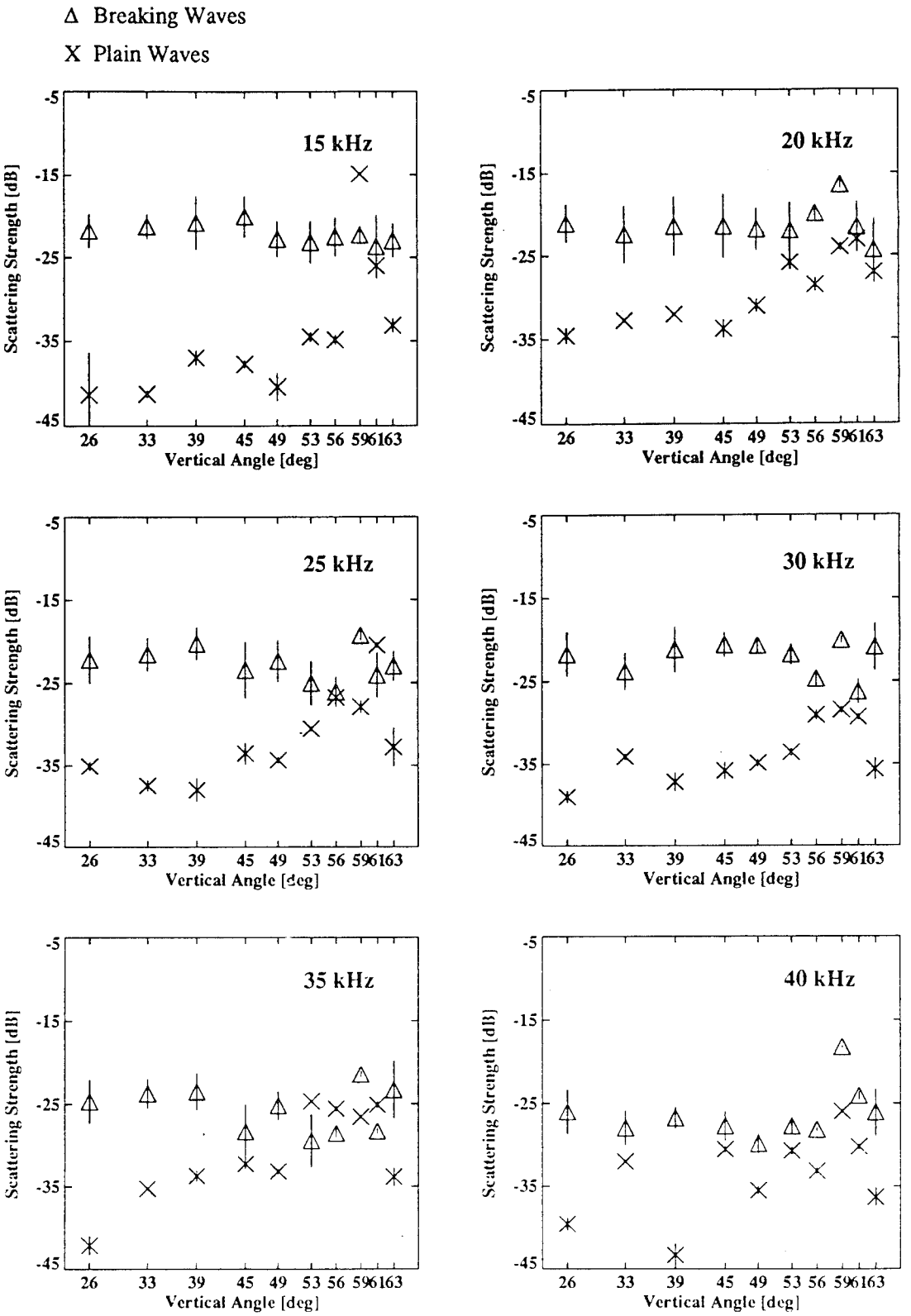

Figure 7. The scattering strength as a function of vertical angle and frequency in the presence (Δ) and absence (×) of breakers.

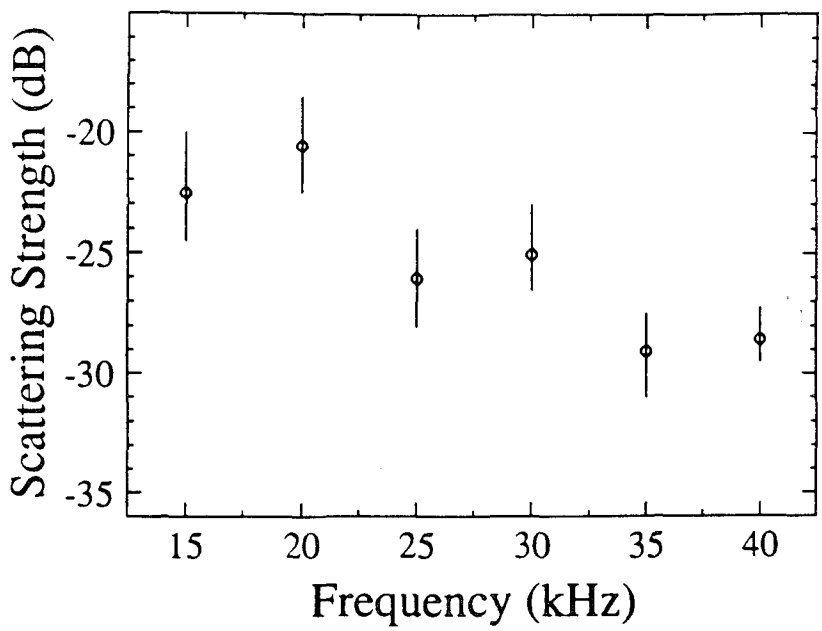

Figure 8. Backscattering strength as a function of frequency from bubble cloud generated by moderate spilling breakers.

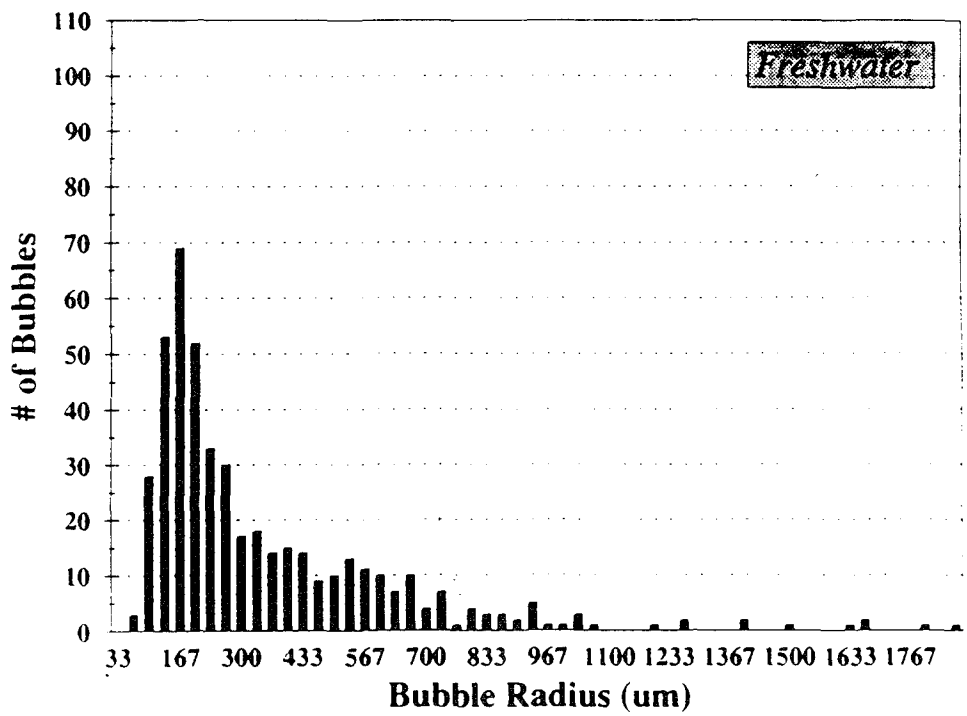

Figure 9. The histogram of the bubble size distribution at the instant when the incident wave scatters off the bubble cloud generated by moderate spilling breakers.

$$c_b^{-2} = (1-\beta)^2 c_\ell^{-2} + \beta^2 c_a^{-2} A + \beta(1-\beta)\left\{\frac{\rho_\ell}{\rho_a} c_a^{-2} A + \frac{\rho_a}{\rho_\ell} c_\ell^{-2}\right\}, \tag{1}$$

where A is given by

$$A = \frac{4\pi}{3\beta} \int_0^\infty \frac{r^3 f(r)\,dr}{1 - \frac{\omega^2}{\omega_0^2(r)} + \frac{2i\omega b(r)}{\omega_0^2(r)}} \quad ; \tag{2}$$

and c is the sound speed with the subscripts a, ℓ, and b referring to air, liquid, and bubbly liquid, respectively, β is the void fraction, ρ is the density, $\omega_0(r)$ and b(r) are resonance frequency and damping constant for a bubble of size r. The function f(r) is the bubble size distribution in a unit volume determined from observations. This model is under development where its results will be compared with backscattering measurements in both fresh and salt water.

TECHNICAL APPROACH

A chief advantage of a controlled experiment is its repeatability where some of the physical parameters could be measured. This enables us to study the complex nature of the sound spectra and acoustic scattering from natural phenomena such as breaking waves. The acoustical and hydrodynamic characteristics of bubble clouds generated by laboratory breakers are being studied both experimentally and theoretically in fresh and salt water. The salinity has a strong effect on the acoustic spectra and sound pressure levels. A theory is being developed where calculation of sound spectra using individual damped oscillations corroborate the gentle spilling breaker measurements where an array of dipole sources for each bubble size is used with inclusion of the frequency–dependent attenuation. Work is continuing on predicting the collective bubble oscillations contribution to the noise spectrum from the more severe breakers. The backscattering model will incorporate the Helmholtz equation in and outside the bubble cloud with an appropriate sound speed in the cloud that will be applicable for incident frequency range and bubble size distribution in the cloud. These observations, both passive and active, along with proper theory will provide considerable insight into the likely source mechanisms for ocean ambient noise and backscattering models in the ocean.

SUBTASK II. BUBBLE–RELATED NOISE IN TURBULENT FLOWS; HYDRODYNAMIC ACTIVATION OF BUBBLES

RESEARCH PROGRESS IN FY94

In order to examine the acoustical behavior of "adult" bubbles encountering a turbulent flow field, we have developed a system that enables us to introduce gas bubbles into the field. The detailed experimental setup and acoustical characteristics are reported.[22] In the progress report for FY 93, it was reported that the turbulent flow field can indeed re–excite and/or breakup an "adult" bubble.

Prediction of the bubble deformation and breakup in a turbulent flow field is a formidable problem, primarily because of the inherent theoretical and experimental difficulties in treating turbulent two–phase flows. Using Stereoscopic Particle Tracking Velocimetry (SPTV), we were able to measure the nearly instantaneous spatial velocity field measurements. It was shown that the rms turbulent intensities have the same general trend and order of magnitude. Therefore, it is reasonable to assume that the flow field under consideration is homogeneous and isotropic and that the eddies in question are in the inertial (–5/3 power) subrange. This assumption is unlikely to be valid in an overall sense though it may be reasonable locally or for the high wavenumbers (small eddies) which are of primary interest. Using these assumptions, the lateral Taylor microscale can be estimated to be

$$\lambda_g \cong \sqrt{\frac{2\overline{u^2}}{\left(\partial u'/\partial r\right)^2}} \quad . \tag{3}$$

The value of λ_g measured at x/D ~ 10 and r ≅ R is about 0.23 cm. Here $\sqrt{\overline{u'^2}}$ is the horizontal rms velocity, x is the distance along the jet, D is the jet diameter, and r is the radial distance. The Kolmogorov microscale η is given by, $\eta = \lambda_g\,(15)^{-1/4}\,(R_{e\lambda})^{-1/2}$, and equal to 3.3×10^{-3} cm, where

$$R_{e\lambda} = \frac{\sqrt{\overline{u'^2}}\,\lambda_y}{\nu} \quad . \tag{4}$$

The lifetime of the turbulent Kolmogorov eddies can be estimated to be around 71 μsec using $\tau_\eta = \eta/\sqrt{\overline{u'^2}}$. The lifetime of the Taylor microscale, $\tau_{\lambda_g} = \lambda_g/\sqrt{\overline{u'^2}}$, is estimated to be about 5.1 msec.

Most of the periods of bubble sizes used in this experiment lie between these two time scales. This implies that the bubble will have enough time to respond to dynamic pressure fluctuations. The eddies with length scales greater than the Kolmogorov scale and much smaller than the Taylor microscale may be responsible for bubble acoustic re-radiation. In general, the fate of a bubble depends on two non-dimensional ratios, the Weber number defined as

$$W_e = \frac{\rho \overline{v'^2}}{\sigma/2R}, \tag{5}$$

and the ratio of length scales $2R/\eta$, where σ is surface tension and R is the radius of the bubble. For our case, $2R >> \eta$, and for high Reynolds numbers the wavenumbers of the energetic eddies and the dissipation range wavenumbers are widely separated. Under these circumstances, Kolmogorov's universal equilibrium theory postulates an inertial subrange at the lower end of the equilibrium range where energy transfer through the spectrum is independent of viscosity and, therefore,

$$\overline{v'^2} = 2.0(2\varepsilon R)^{2/3} \ , \tag{6}$$

where ε is the energy dissipation per unit mass and time. Under these conditions, Eq. (5) will have a new form,

$$(W_e)_{critical} = 6.36[(\rho/\sigma)\varepsilon^{2/3}R^{5/3}] \ . \tag{7}$$

Since the small–scale structure of turbulence at large Reynolds numbers is always approximately isotropic,

$$\varepsilon = 15\nu\left(\frac{\rho\overline{u'^2}}{\lambda_g^{\ 2}}\right) \ . \tag{8}$$

To obtain the lowest number at which bubble deformation and subsequent acoustic radiation will occur, we use the maximum Reynolds shear stress $\rho\overline{u'^2}$ in a region where the "adult" bubble may be re-excited. The resulting critical Weber number is about 0.52. The critical number at which the bubble breaks up is about 1.10.

We have already begun developing a model that includes the bubble dynamics encountering a turbulent flow field. The model under development assumes that the viscous effects are negligible (i.e., $R_e = Ru/\nu >> 1$), the bubble deformation is small, and a bubble does not alter the mean velocity. With these assumptions, the governing equation for the bubble dynamics can be written as

$$\frac{\partial \xi_{n,m}}{\partial t} + (n+1)\phi_{n,m} = 0, \tag{9}$$

and

$$\frac{\partial \phi_{n,m}}{\partial t} - \frac{\omega_n^2}{n+1}\ \xi_{n,m} = (2n+1)\ \langle\ Y_{n,m} \cdot G'\ \rangle, \tag{10}$$

where ξ is the bubble radius, the potential function $\phi_{n,m}$ is related to the turbulent energy containing broader spectrum of eddies, $Y_{n,m}$ is the Legendre polynomials, G' is related to fluid dynamics acting on bubbles, and ω_n is the frequency of the bubble. This theory is also under development where we will take second order approximations of non–spherical bubbles to predict monopole acoustic radiation to the far field and ultimately results will be compared with experimental observations.

REFERENCES CITED

1. B.R. Kerman (ed.), "Natural mechanisms of surface-generated noise in the ocean," in *Sea Surface Sound* (Kluwer, Dordrecht, The Netherlands, 1988).

2. B.R. Kerman, (ed.), "Natural mechanisms of surface-generated noise in the ocean," in *Natural Physical Sources of Under Water Sound* (Kluwer, Dordrecht, The Netherlands, 1993).

3. M.J. Buckingham and J.R. Potter, *Sea Surface Sound '94,* Lake Arrowhead, CA, March, 1994.

4. V.O. Knudsen, R.S. Alford, and J.W. Emling, "Underwater ambient noise," *J. Mar. Res.,* **7**, 410-429 (1948).

5. H. Medwin and A.C. Daniel, "Acoustical measurements of bubble production by spilling breaker," *J. Acoust. Soc. Am.,* **88**, 408-412 (1990).

6. L. Ding and D.M. Farmer, "On the dipole acoustic source level of breaking waves," *J. Acoust. Soc. Am.,* in press.

7. A. Prosperetti, "Bubble-related ambient noise," *J. Acoust. Soc. Am.*, **84**, 1042-1054 (1988).

8. D.M. Farmer and L. Ding, "Coherent acoustical radiation from breaking waves," *J. Acoust. Soc. Am.*, **92 (1)**, 397-402, 1992.

9. G.E. Updegraff, "In situ investigation of sea surface noise from a depth of one meter, Ph.D. thesis, University of California, San Diego, 1989.

10. R.M. Kennedy, "Sea surface dipole sound source dependence on wave–breaking variables," *J. Acoust. Soc. Am.*, **91**, 1974-1982 (1992).

11. W.M. Carey, J.W. Fitzgerald, E.C. Monahan, and Q. Wang, "Measurements of the sound produced by a tipping trough with fresh and salt water," *J. Acoust. Soc. Am.*, **93**, 3178-3142 (1992).

12. A.R. Kolaini, R.A. Roy, L.A. Crum, and Y. Mao, "Low–frequency underwater sound generation by impacting transient cylindrical water jets," *J. Acoust. Soc. Am.*, **94** 2809-2820 (1993).

13. A.R. Kolaini, R.A. Roy, and D. Gardner, "Low–frequency acoustic emissions in fresh and salt water," *J. Acoust. Soc. Am.*, **96 (3)**, 1765-1774 (1994).

14. W.M. Carey and D.G. Browning, "Low–frequency ocean ambient noise: measurements and theory," in *Sea Surface Sound,* edited by B.R. Kerman (Kluwer, Dordrecht, The Netherlands, 1997), pp. 361-376.

15. H. Oguz, "A theoretical study of low–frequency oceanic ambient noise," *J. Acoust. Soc. Am.*, **95**, 1895-1912 (1994).

16. F.S. Henyey "Acoustic scattering from ocean microbubble plumes in the 100 Hz – 2 kHz region," *J. Acoust. Soc. Am.*, **90**, 399-405, (1991).

17. B.E. McDonald, "Echoes from vertically striated subresonant bubble clouds: a model for ocean surface reverberation," *J. Acoust. Soc. Am.*, **87**, 617-622 (1990).

18. A.R. Kolaini and L.A. Crum, "Observations of underwater sound fromlaboratory breaking waves and the implications concerning ambient noise in the ocean," *J. Acoust. Soc. Am.*, **96 (3)**, 1755-1765 (1994).

19. P.B. Dandenault, "The measurements of the scattering of sound from laboratory–generated breaking waves," M.S. Thesis, University of Mississippi, 1994.

20. M.R. Lowen and W.K. Melville, "A model of the sound generated by breaking waves," *J. Acoust. Soc. Am.*, **90 (4)**, 2075-2080 (1991).

21. K. Sarkar and A. Prosperetti, "Backscattering of underwater noise by bubble clouds," *J. Acoust. Soc. Am.*, **93 (6)**, 3128-3138 (1993).

22. A.R. Kolaini, "Acoustic characterization of an adult bubble injected into a fully developed turbulent flow field," submitted to *J. Acoust. Soc. Am.*, 1994

PUBLICATIONS AND PRESENTATIONS FOR FY94

A. Published papers in Referred Journals and Edited Conference Proceedings

1. A.R. Kolaini, L.A. Crum, and R.A. Roy "Acoustically active bubble production by capillary-gravity waves," *J. Acoust. Soc. Am.*, **95(4)**, 1913-1921 (1994).

2. A.R. Kolaini and M.P. Tulin, "Experimental studies of unsteady three-dimensional spilling breaking waves," ASME, submitted to *J. of OAME*, 1994.

3. Y. Yao, M.P. Tulin, and A.R. Kolaini, "Theoretical and experimental studies of three-dimensional wavemaking in narrow tanks, including nonlinear phenomena near resonance, " *J. of Fluid Mech.,* in press.

4. A.R. Kolaini, R.A. Roy, and D. Gardner, "Low-frequency acoustic emissions in fresh and salt water," *J. Acoust. Soc. Am.*, **93(6)**, 1766-1772 (1994).

5. A.R. Kolaini and L.A. Crum, "Observations of underwater sound from laboratory breaking waves and the implications concerning ambient noise in the ocean," *J. Acoust. Soc. Am.*, **93(6)**, 1755-1765 (1994).

6. A.R. Kolaini, P. Dandenault, and A.R. Ruxton, "Passive and active acoustical measurements of laboratory breaking waves," in the Proceedings of the 4th Sea Surface Sound, Los Angeles, CA, March 1994.

7. A.R. Kolaini, C. You, and P.D. Dandenault, "Measurements of the backscattering of underwater sound from laboratory breaking waves," in the proceedings of the Western Pacific Regional Acoustics Conference V, Seoul, Korea, August 1994.

8. A.R. Kolaini, H.N. Oguz, and A. Prosperetti, "Impact of cylindrical water jets on water surfaces, " submitted to the *J. Fluid Mech.,* 1994.

9. A.R. Kolaini, S.K. Sinha, and V.P. Rajendran, "Interaction of bubbles with turbulent flow: Particle tracking and flow field characterization," in the Proceedings of the *Twentieth Symposium on Naval Hydrodynamics*, June 1994.

10. A.R. Kolaini, "Acoustic characterization of an adult bubble injected into a fully developed turbulent flow field," submitted to *J. Acoust. Soc. Am.,* 1994.

B. Papers Presented before Professional Organizations

1. A.R. Kolaini, P. Dandenault, and A.R. Ruxton, "Passive and active acoustical measurements of laboratory breaking waves," presented at the 4th Sea surface Sound, Los Angeles, CA, March 1994.

2. A.R. Kolaini, C. You, and P.D. Dandenault, "Measurements of the backscattering of underwater sound from laboratory breaking waves," presented at the Western Pacific Regional Acoustics Conference V, Seoul, Korea, August 1994.

3. A.R. Kolaini, S.K. Sinha, and V.P. Rajendran, "Interaction of bubbles with turbulent flow: Particle tracking and flow field characterization," presented at the Twentieth Symposium on Naval Hydrodynamics, June 1994.

4. P.B. Dandenault, and A. R. Kolaini, "Measurements of the backscattering of sound from laboratory breaking waves," presented at the 128th Meeting of the Acoustical Society of America, Austin , TX, November, 1994.

5. A. R. Kolaini, "Acoustic characterization of laboratory breaking waves in fresh and salt water," presented at the 128th Meeting of the Acoustical Society of America, Austin, TX, November, 1994.

6. H.A. Oguz, A. Prosperetti, and A.R. Kolaini, "A simplified description of the impact of a liquid mass on a liquid surface," APS Fluid Dynamics Conference, Atlanta, Georgia, November 1994.

EXPERIMENTAL INVESTIGATIONS OF AN ACOUSTIC SOLITON

ABSTRACT

The purpose of this research is to generate and observe nonlinear Schrödinger solitons in an acoustic waveguide. These waves, which have not yet been observed, are theoretically characterized by a standing wave motion in the transverse direction, an exponential self-localization along the waveguide, and a speed of propagation that can have any value that is small compared to the speed of sound.

We are motivated to pursue this research for several fundamental reasons. There are few observations of bulk solitons at the present time, and so the perturbative theories remain largely untested. Our observation would be the first of acoustic solitons in a single-phase medium. The existence of these waves in a physical system and the degree to which they remain intact are open questions in the dynamics of soliton-like waves in nearly-integrable systems. For example, these solitons may exist at speeds greater than the speed of sound, which is beyond the range of the perturbation theory. They would thus be "tachyons" in sound. Our proposed physical system could be a probe of the unexplained phenomenon of soliton shedding, and could lead to the observation of a two-dimensional self-localized state.

Possible applications of this acoustic soliton include the probing and possible cleaning of conduits, (e.g., oil lines, nuclear power cooling lines, and blood arteries). Another possible application is the use of these solitons as localized sources of sound that travel down bore holes in the earth, to be utilized in the search for oil and natural gas by the method of acoustical tomography.

OBJECTIVE

The initial objective of this research is to empirically find an acoustic medium that yields a resonance frequency that significantly *decreases* as the response amplitude is increased. There is

currently only a small amount of literature regarding this subject as it pertains to acoustics, and this literature is contradictory. The next objective is to construct a waveguide that contains the acoustic medium, and to then generate and observe an acoustic soliton of the nonlinear Schrödinger type.

BACKGROUND

Nonlinearities give rise to fundamentally different behavior of waves as compared to the linear level. A dramatic example of this is a *soliton,* which is a self- localized wave of permanent shape that collides elastically with other waves; it is a wave that acts as a particle. Although solitons were first observed and studied in the 1830s by naval architect John Scott Russell,[1] they did not receive substantial attention until the 1960s when Zabusky and Kruskal[2] numerically discovered the elastic collisional property. The first application of solitons is planned to be implemented at the end of this decade, when fiber optic solitons will be employed in transatlantic telecommunication lines.[3]

Our interest in solitons began with the observation of a standing localized surface wave in a long uniform channel of deep liquid.[4] Steady state motion is achieved by vertically oscillating the channel. In the frame of reference of the channel, the liquid is motionless except in a relatively small region where it sloshes transverse to the channel (Fig. 1a). The state is referred to as a *breather.* The underlying approximate description was found to be a nonlinear Schrödinger (NLS) equation,[5] which describes these states as amplitude modulations of the cutoff mode (in which the liquid sloshes transversely with uniform amplitude). The breather can be understood as a self-trapped state which can occur because the oscillations soften, i.e., the resonance frequency decreases for greater response amplitudes. In contrast, the oscillations harden for a sufficiently shallow liquid, and consequently a *cutoff kink* soliton can exist.[6,7] In this state, the liquid sloshes at constant amplitude transverse to the channel in two extended regions, with a 180° phase difference between the two regions (Fig. 1b). The cutoff kink is the localized transition region that connects the motion in the two regions. Our observations showed that the surface wave kink can exist at amplitudes substantially beyond which the perturbation theory is valid, indicating that the state is a more general phenomenon than the theory predicts.

Experiments we performed with a mechanical lattice, backed by numerical simulations, have yielded analogous breather and kink solitons and, more importantly, fundamentally new types of localized states.[8,9] These are *domain walls,* which are localized transition regions that connect two standing wave regions of different wavenumber, and *noncutoff kinks,* which connect two standing wave regions of the same wavenumber with a difference in spatial phase. These new states cannot be described by an NLS equation. Our observations have prompted several new theories of the

states. In one, modulations in both amplitude and wavenumber are allowed.[10] Further experimentation led to our observation that *propagating* solitons can be spontaneously shed at a driven point (e.g., boundary) of a lattice if the drive parameters are in the appropriate range.[11,12] These solitons are essentially moving breathers. They can potentially exist in a cutoff mode of any system if the nonlinear nature of the mode causes the finite-amplitude motion to shift the frequency *outside* the linear propagation band. As discussed above, such is the case for cross surface gravity wave modes in a channel of deep liquid, and propagating breathers have indeed been observed in this system.[13,14]

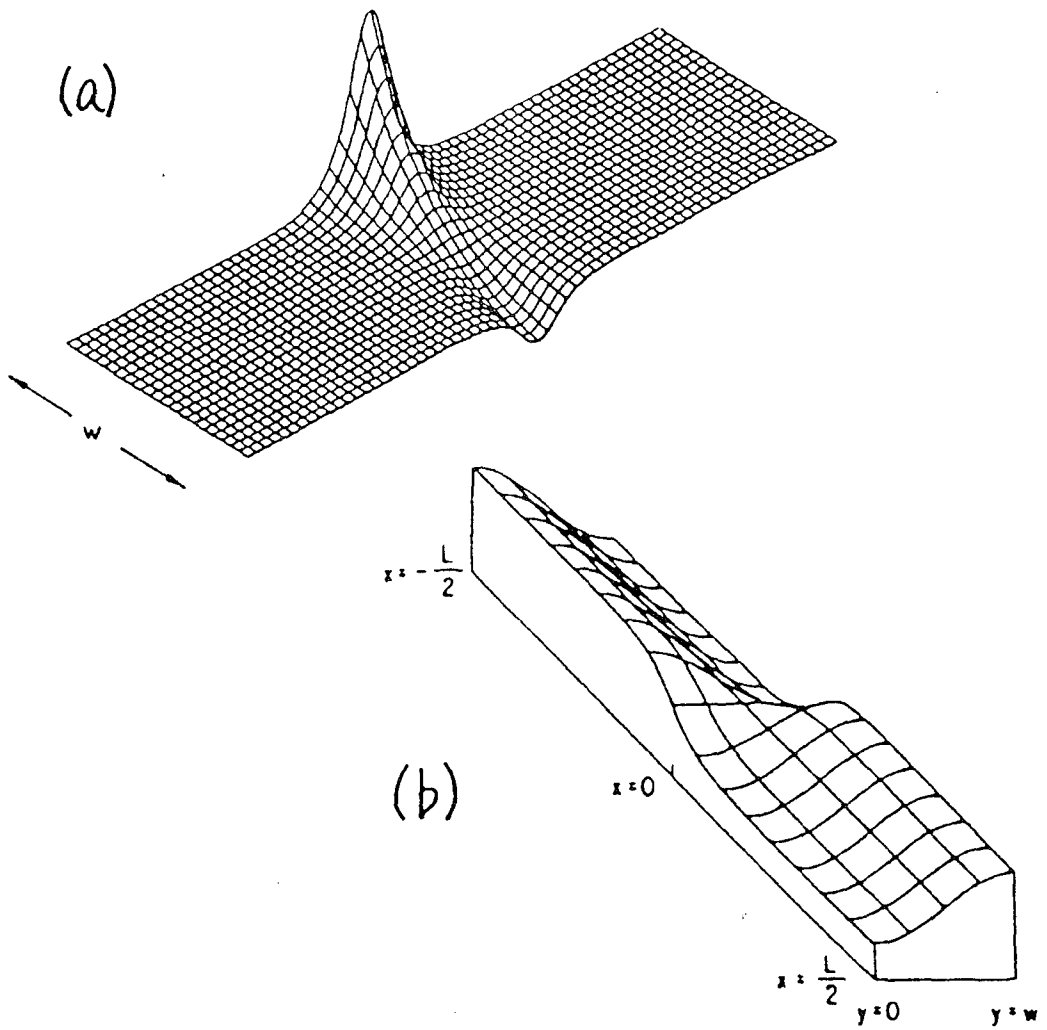

Figure 1. Steady state nonpropagating solitons on the surface of a liquid in a channel: (a) breather, in the case of a deep liquid, and (b) cutoff kink, in the case of a shallow liquid. The surface oscillates up and down.

For the system of a fluid that fills a long tube, the acoustic cross modes are predicted to harden in the case of a gas and soften in the case of a liquid.[15] (However, see the discussion in the Technical Approach section.) Hence, we expect that propagating breathers can exist in the liquid case. Because they involve oscillatory motion in a bulk medium, we refer to these states as *acoustic solitons.* To our knowledge, the scientific literature does not contain any observations of acoustic NLS solitons in a physical system. In fact, only two types of solitons in bulk media have been observed: optical solitons in fibers (as mentioned above), and Korteweg-de Vries solitons in liquid-gas mixtures.[16]

As a theoretical illustration of acoustic solitons, consider the simple model equation of motion

$$\partial^2\varphi/\partial t^2 - c^2\nabla^2\varphi = -\alpha\nabla^2\varphi^3 \ , \qquad (1)$$

where φ is the field variable (e.g., the pressure deviation), c is the speed of linear waves, α is the nonlinear coefficient, and $\nabla^2 = \partial^2/\partial x^2 + {}^2/\partial y^2$. In this model, the nonlinearity acts to resonantly drive the harmonics of a wave, resulting in infinite amplitudes of the harmonics. This problem is not relevant for our purposes because in a real system the dissipation will prevent this blow-up. If x is the longitudinal coordinate, y the transverse coordinate, and w is the width of the wave guide, we seek a solution of the form

$$\varphi = A(x,t)\cos(ky)\exp(i\omega t) + \text{c.c.} + \ldots \ , (2)$$

where the transverse wavenumber is $k = \pi/w$ for the fundamental mode, the amplitude A(x,t) is a weakly-nonlinear slowly-varying complex function, c.c. denotes the complex conjugate, and the ellipsis signifies higher harmonics. Substituting this into the equation of motion, and making the approximations, leads to a nonlinear Schrîdinger equation that has the propagating breather solution[17]

$$A(x,t) = b_o\,\mathrm{sech}[b_1(x-vt)/c]\exp(-iv\omega x/c^2) \ , \qquad (3)$$

where the velocity v is a free parameter, and where $b_o^2 = 8b_1^2/9\alpha k^2$, $b_1^2 = \omega_o^2 - \omega^2(1-v^2/c^2)$, and $\omega_o = ck$. Note that this solution exists only for $a > 0$, which corresponds to a system with a softening nonlinearity. The full solution represents a traveling disturbance that is transversely oscillating, exponentially localized in the longitudinal direction, and propagating with velocity v.

It is interesting that the solution exists not only for small values of v/c but also for larger values, including $v/c > 1$. Hence, there is the possibility of an acoustic "tachyon" here. Lack of smallness of v/c violates the assumptions of the perturbation expansion leading to the solution, but

the disturbance may still remain intact. This possible robustness of the localized state would be of important interest both fundamentally and practically.

RESEARCH PROGRESS IN FY94

The first problem, which has consumed our efforts during the first year of this research, is the identification of an acoustic medium that softens; i.e., where the resonance frequencies significantly decrease with increasing response amplitude. As explained in the Background section, this softening is necessary for the NLS solitons to exist, and corresponds to the sign of the effective overall nonlinear standing wave coefficient. There is currently only a small amount of acoustical literature on the subject. Aranha *et al.*[15] derive standing wave nonlinear coefficients which imply that gases harden and liquids soften for azimuthally symmetric modes in a cylindrical geometry. If numbers are substituted into the theory, however, we find that a 1.0 atm pressure swing in water is predicted to cause a frequency shift of only 1 part in 10^{10}! This is unsuitable for our purposes because the effects of even very small geometric nonuniformities will dominate the desired nonlinear effect.

We decided to experimentally test the Aranha prediction, for several reasons. First, the theory is complicated and thus could be in error. Second, standing wave nonlinear coefficients for other liquids are not known, and our apparatus would easily accommodate many other liquids. In particular, it is known that the traveling wave nonlinear coefficients for bubbly liquids can be very large.[18] Although the connection between standing and traveling wave nonlinear coefficients for sound has not yet been established, it is expected that they are of the same order of magnitude.

Two resonators have been built: an open styrfoam-lined parallelepiped with inner dimensions $4 \times 8 \times 6$ inches, and a sealed 1 inch thick brass cylinder with inner diameter 4 inches and inner length 6 inches. Measurements of resonances in water have been carried out in both resonators. The styrofoam resonator yielded a pressure node boundary condition, as expected. The brass resonator yielded an approximate pressure antinode boundary condition. (Thick brass was employed to help achieve this boundary condition.) Due to the immediate availability, a Bruel & Kjaer 8105 hydrophone was used to drive various modes in the resonators. We observed no bending (i.e., neither softening nor hardening) of the frequency response curves for maximum response amplitudes of 0.0025 atm (168 dB re 1 (Pa). We then built a piezoelectric stack to act as a radial driver on the axis of the brass cylinder. We observed no bending in regular tap water up to amplitudes of 0.010 atm (180 dB), where cavitation occurred. We also observed no bending of degassed water for maximum response amplitudes of 0.020 atm (186 dB). In order to increase the cavitation threshold, we modified the piezoelectric stack and the sealed brass resonator system such that the system could be pressurized. Under 0.5 atm of static pressure, we suppressed the

cavitation of the tap water but observed no bending for maximum response amplitudes of 0.020 atm (186 dB).

We then turned our attention to bubbly liquids. Carbonated water under a pressure of 0.5 atm was investigated first. Sufficient time after pouring and closing the system was allowed to pass so that the system reached equilibrium. However, sweeping the drive frequency at high drive amplitude, which is necessary to establish nonlinear tuning curves, was found to alter the system. The effect of driving at high amplitudes evidently changes the amount of gas in solution, thus affecting the size and number of bubbles present and thus the void fraction of bubbles. The system required some time to relax back to equilibrium, where low amplitude measurements became reproducible. The altering of the equilibrium of the system by high amplitude drives was unacceptable for our purposes. We thus concluded, although incorrectly at that time (Oct. 94), that any bubbly liquid we use in the future must be such that the bubbles are frozen in position.

With the aim of studying a frozen bubble system, we experimented with Agar,[19] a gel-like substance in which fixed bubbles can be produced by pressurizing it at 5 atm for 24 hours as it gels. For our measurements, we consistently prepared an Agar/water mixture at 1.75% by volume. The measurements were complicated by the fact that the gel coupled low frequency noise (20 Hz) into the Bruel & Kjaer 8103 hydrophone. Furthermore, as a result of being necessarily exposed to the 80°C required to dissolve the Agar powder, our piezoelectric stack cracked to release whatever stress it had been under. Another complication of the Agar system is due to the fact that as time elapses the gel shrinks and thus looses physical contact with the transduction devices. Our frequency sweeps were carried out within less than 24 hours of pouring and showed no bending.

We then decided to again experiment with dynamic bubbles, but now injected via 27-gauge hypodermic needles placed at the bottom endplate of the cylindrical brass resonator. The bubble radius is fixed at approximately 1.2 mm by the size of the needles. The bubbles are produced by a continuous flow of nitrogen, and rise to the top of the resonator where the gas is released when the bubbles leave the liquid. Because we desired rigid boundary conditions, we designed a top plate with small holes from which the air would escape but which would act as a containment for the water. We did not consider the fact that this escape plate with small holes would act more as a pump than as a release, altering continuously the liquid level inside the resonator cavity. We thus switched from closed-closed resonator configuration to a closed-open resonator configuration, which has the important additional advantage of allowing the modal structure to be probed with a small movable hydrophone. We used a home-made hydrophone that was previously constructed by Dr. Thomas Harley of NCPA.

Figure 2 shows frequency response curves for the fundamental mode of the bubbly-liquid resonator. The decrease of the resonance frequency for greater drive amplitudes is precisely what

is required for the soliton we wish to observe. However, we discovered that the shift in frequency was a result of a small gradual increase in the gas flow rate during the time the data was gathered. The resultant increase in the void fraction caused the decrease in resonance frequency. We installed a better flow meter and the shifts in resonance frequency disappeared.

We have placed strong emphasis in the research of a bubbly liquid because in case of observing softening of longitudinal resonances we would be in a position to do theory with a Burgerís-type equation to explain the bending.[22] We have identified (by mapping as a function of position) and measured the fundamental longitudinal resonance as a function of drive amplitude and as a function of bubble void fraction (0.01% to 0.5%) for our toroidal resonant cavity (inner diameter 1.5 in., outer diameter 4 in., and height 6 in.). We have not observed any bending at maximum response levels of 0.02 atm (166 dB *re* 1 μPa). One problem we encountered was that the noise due to the bubble generation is not negligible, so we now use a lock-in amplifier and sweep very slowly across the resonance. Also, the quality factor Q of the resonance is typically only 6 to 7. We are currently building a piston-drive system[23] to be able to reach much greater pressure deviations.

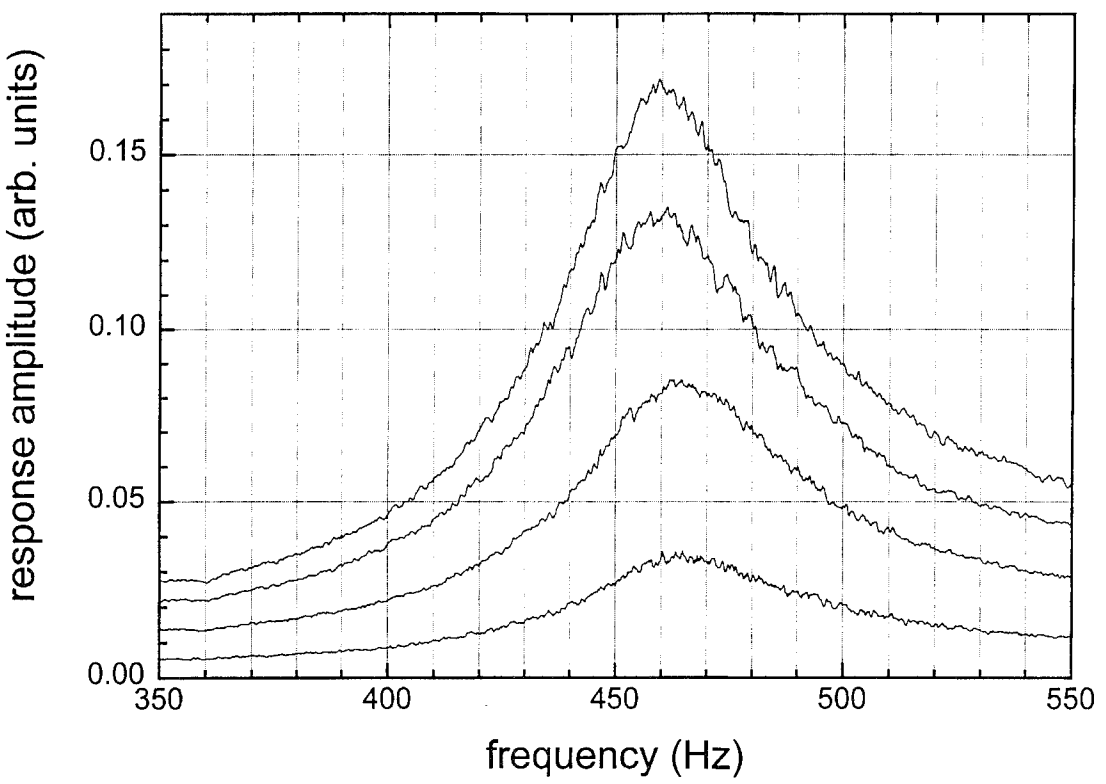

Figure 2 Frequency response curves for the fundamental mode of a bubbly-liquid resonator. (Each curve corresponds to a constant drive amplitude.)

We have also been investigating *single-bubble sonoluminescence* (SL), in which light is emitted from a bubble that is trapped at a pressure antinode of a standing wave in water.[24,25] The mechanism of the light emission is not yet understood. Many of the theories require that the gas in the bubble be at least partially ionized. We thus conjectured that placing a SL bubble in a magnetic field could reveal the extent of ionization and possibly break the isotropy of the emission. Back-of-the-envelope calculations suggested that a magnetic field of roughly 1 T would have a significant effect. We performed an experiment with an SL bubble in magnetic fields up to 0.5 T, but found no change in intensity of the emitted light.

A magnetic field of roughly 1 T should produce a spectral spike in the microwave region. This prompted us to consider microwave emission of SL. Most of the SL spectrum remains hidden because the dielectric properties of water permit only a small window of frequencies to propagate. This spectral drape includes wavelengths up through ultraviolet, and from infrared to millimeter values. However, our analysis has revealed a small region in the 1-5 GHz region that can be measured using well established techniques of microwave radiometry. Recent measurements of the cosmic microwave background with standard off-the-shelf equipment have resolved the differential power to one tenth of a femtowatt.[26] We are currently developing and characterizing a radiometer to measure the microwave power emission of an SL bubble.

The current quantitative theories of SL involve thermal bremsstrahlung,[27] blackbody,[28] collision induced emission,[29] and Casimir light.[30] Theorists have managed to make each of these fit the SL data in the visible region of the spectrum. We have examined the theories and extrapolated their predictions into the microwave region, where a divergence of twenty orders of magnitude occurs (Fig. 3). Bremsstrahlung is predicted to yield the largest spectral density in the microwave region, with a peak power emission in a 1 GHz band of over 10 nW which well above the noise threshold of many detectors. Our measurements should reduce the number of possible theories, hopefully to only one.

We have constructed a large (1 liter) spherical cell and developed the appropriate instrumentation to seed and maintain a sonoluminescence bubble for several hours. We have also constructed a vacuum-tight cylindrical cell to be used with bubbles doped with a noble gas such as xenon. In addition we have constructed a manifold for degassing the water and then regassing the water with a desired gas mixture. We are currently measuring the impedance of a microwave antenna in water. This will allow us to set an upper limit on the noise of our radiometer.

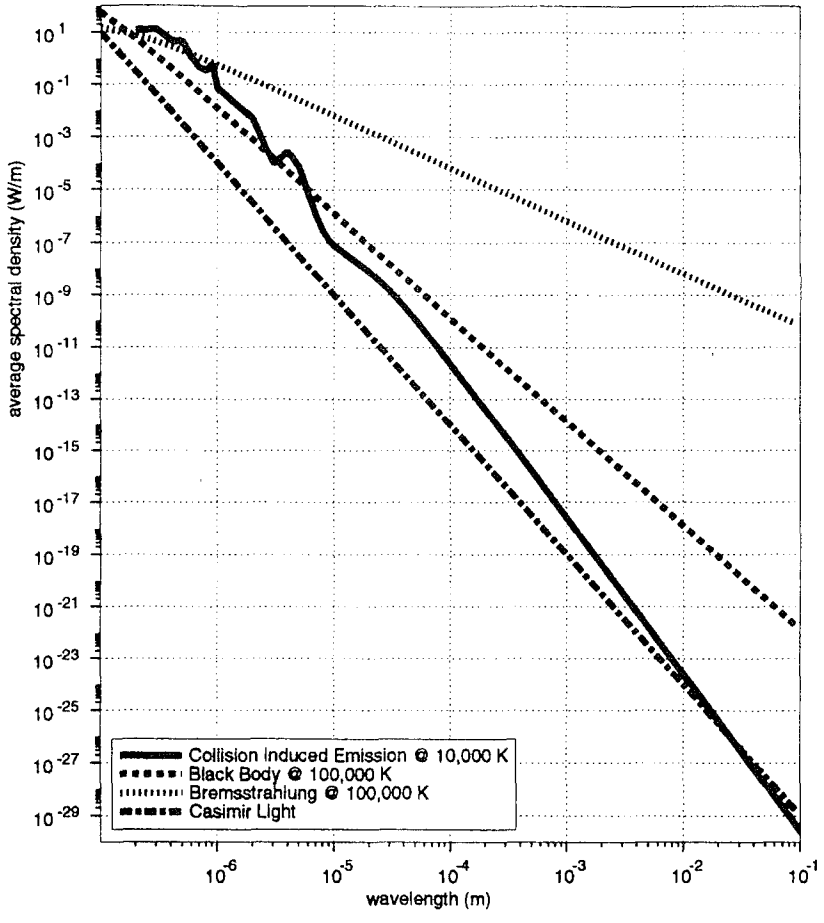

Figure 3. Sonoluminescence spectral density according to different theories. All theories agree in the visible region (roughly 10-7 m), but most strongly disagree in the microwave region (roughly 10-1 m).

REFERENCES CITED

1. R. Dodd, J. Eilbeck, J. Gibbon, and H. Morris, *Solitons and Nonlinear Wave Equations* (Academic, New York, 1982).

2. N. Zabusky and M. Kruskal, "Interaction of 'solitons' in a collisionless plasma and the recurrence of initial states," *Phys. Rev. Lett.*, **15**, 240-243 (1965).

3. L. F. Mollenauer, J. P. Gordon, and S. G. Evangelides, "Multigigabit soliton transmissions traverse ultralong distances," *Laser Focus World*, November 1991, 159-170.

4. J. Wu, R. Keolian, and I. Rudnick, "Observation of a nonpropagating hydrodynamic soliton," *Phys. Rev. Lett.*, **52**, 1421-1424 (1984).

5. A. Larraza and S. Putterman, 1984b: "Theory of nonpropagating surface wave solitons," *J. Fluid Mech.*, **148**, 443-449.

6. B. Denardo, W. Wright, S. Putterman, and A. Larraza, "Observation of a kink soliton on the surface of a liquid," *Phys. Rev. Lett.*, **64**, 1518-1521 (1990).

7. Bruce Denardo, *Observations of nonpropagating oscillatory solitons* (Ph.D. dissertation, Department of Physics, University of Califonia, Los Angeles, CA, 1990).

8. B. Denardo, B. Galvin, A. Greenfield, A. Larraza, S. Putterman, and W. Wright, "Observations of localized structures in nonlinear lattices: Domain walls and kinks," *Phys. Rev. Lett.*, **68**, 1730-1733 (1992).

9. Brian Galvin, *Kinks in Nonlinear Lattices* (M.S. thesis, Department of Physics, Naval Postgraduate School, Monterey, CA, 1992), advisors: Bruce Denardo and Andrés Larraza.

10. B. Denardo, A. Larraza, S. Putterman, and P. Roberts, "Nonlinear theory of localized standing waves," *Phys. Rev. Lett.*, **69**, 597-600 (1992).

11. Mary Atchley, *Observations of Solitons in a Nonlinear Lattice* (M.S. thesis, Department of Physics, Naval Postgraduate School, Monterey, CA, 1992), advisor: Bruce Denardo.

12. Cleon Walden, *Breathers in Nonlinear Lattices* (M.S. thesis, Department of Physics, Naval Postgraduate School, Monterey, CA, 1992), advisors: Bruce Denardo and AndrÇs Larraza.

13. E. Kit, L. Shemer, and T. Miloh, "Experimental and theoretical investigation of nonlinear sloshing waves in a rectangular channel," *J. Fluid Mech.*, **181**, 265-291 (1987).

14. Yitao Yao, Marshall P. Tulin, and Ali R. Kolaini, "Theoretical and experimental studies of three-dimensional wavemaking in narrow tanks, including nonlinear phenomena near resonance," to appear in *J. Fluid Mech.* (1994).

15. J. A. Aranha, D. K. P. Yue, and C. C. Mei, "Nonlinear waves near a cut-off frequency in an acoustic duct – a numerical study," *J. Fluid Mech.*, **121**, 465-485 (1982).

16. V. Kuznetsov, V. Nakoryakov, B. Pokusaev, and I. Shreiber, "Propagation of perturbations in a gas-liquid mixture," *J. Fluid Mech.*, **85**, 85-96 (1978).

17. A. Larraza and S. Putterman, "Theory of nonpropagating hydrodynamic solitons," *Phys. Lett.*, **103A**, 15-18 (1984).

18. Junru Wu and Zhemin Zhu, "Measurements of the effective nonlinearity parameter B/A of water containing trapped cylindrical bubbles," J. *Acoust. Soc. Am.*, **89**, 2634-2639 (1991).

19. S. Daniels, D. Blondel, L. A. Crum, G. R. ter Haar, and M. Dyson, "Ultrasonically induced gas bubble production in Agar based gels: Part I, Experimental investigation," *Ultrasound in Med. and Biol.*, **13**, 527-539 (1987).

20. W. Ellermeier, "Acoustic resonance of cylindrically symmetric waves," *Proc. Roy. Soc. Lond.*, **A445**, 181-191 (1994).

21. Andrés Larraza and Bruce Denardo, "Absorption of sound by noise in one dimension," *J. Acoust. Soc. Am.*, **91** (2), 2330 (1992).

22. D. G. Crighton, A. P. Dowling, J. E. Ffowcs Williams, M. Heckl, and F. G. Leppington, *Modern Methods in Analytical Acoustics* (Springer-Verlag, New York, 1992), Ch. 21.

23. Stanley A. Cheyne and Carl T. Stebbings, "Phase velocity measurements in bubbly liquids using a fiber optic interferometer," *J. Acoust. Soc. Am.* **97**, 1621-1624 (1995).

24. Lawrence Crum, "Sonoluminescence," *Phys. Today*, Sep. 1994, 22-29.

25. Seth J. Putterman, "Sonoluminescence: Sound into light," *Sci. Am.*, Feb. 1995, 46-51.

26. G. Smoot et al., "COBE Differential Microwave Radiometers: Instrument Design and Implementation," *Astrophys. J.* **360**, 685-695 (1990).

27. C.C. Wu and P.H. Roberts, "A model of sonoluminescence," *Proc. Roy. Soc. Lond. A.* **445**, 323-349 (1994).

28. Robert Eisberg and Robert Resnick, *Quantum Physics of Atoms, Molecules, Solids, Nuclei, and Particles*, 2nd ed. (Wiley, New York, 1985), pp. 6-21.

29. Lothar Frommhold and Anthony A. Atchley, "Is sonoluminescence due to collision-induced emission?," *Phys. Rev. Lett.* **73**, 2883-2886 (1994).

30. Julian Schwinger, "Casimir light: The source," Proc. *Natl. Acad. Sci. U.S.A.* **90**, 2105-2106 (1993).

ATTENUATION MECHANISMS IN SEDIMENTS

ABSTRACT

During the past year, the attenuation of sound in tubes which results from mass transfer was modeled. The model is based on the physics of sound attenuation in atmospheric fogs. An acoustic surface impedance measurement of a tubular-porous material was made. The measured data show a strong effect due to mass transfer.

INTRODUCTION

The biogeodynamics of shallow water ocean sediments is the source of the gas bubbles that exist in these sediments. Acoustic sub-bottom seismic reflectivity measurements of ocean sediments show gas horizons within one-half meter of the sediment-water interface.[1] Additionally, x-ray CT scans show images of individual bubbles of 0.1 cm size within these sediments. Current systems are limited to 0.1 cm resolutions. Others[2] are investigating sources and composition of gas bubbles and dissolved gas in ocean sediments. Low-grazing angle acoustic back scattering from a gassy sediment[3] requires knowledge of the acoustic absorption coefficients in the sediment. Chitiros has included the Biot slow wave number in back scattering predictions and is currently attempting to incorporate gassy sediment effects into these calculations.

We proposed to study attenuation mechanisms in addition to the Biot viscous drag and thermal conductivity. This effort has focused on acoustic condensation or mass transfer of the water vapor constituent in saturated vapor bubbles. In the first year (1993), we identified attenuation mechanisms alternative to grain slippage and squeeze film fluid motion. One such mechanism was mass transfer. The physics of mass transfer in fogs has been used to model sound absorption in a cylindrical tube. We have also completed an experiment which demonstrates this effect.

RESEARCH PROGRESS IN FY94

The physics of acoustic condensation or mass transfer is well established for atmospheric fogs. A fog consists of spherical droplets of water immersed in a saturated water-vapor/air mixture. A gassy sediment is the inverse of the fog. The sediment consists of gas bubbles saturated with water vapor and gas immersed in a liquid/solid skeleton.

When an acoustic wave compresses a volume element of a fog, the equilibrium concentration of water vapor molecules is perturbed and can return to equilibrium via mass transfer or condensation of water vapor to the droplet surface. Acoustic evaporation can also occur. For energy loss, the latent heat of condensation/evaporation must be conducted away in a time period on the order of the acoustic cycle.

In a sediment, the acoustic compression causes water vapor molecules in the gas bubble to condense (evaporate) at the gas/water interface. The physics of mass transfer in the fog or sediment is the same. In both cases fundamental equations of mass, momentum, and energy are conserved. Additionally, the equilibrium saturation vapor pressure is expressed in terms of the temperature through the Clausius-Clapeyron equation. The vapor/gas mixture is assumed to obey the ideal gas law.

For the fog, we have re-derived the fundamental equations from first principles and accomplished the linearization of these equations. A simpler problem consisting of pure water vapor and water droplets has been set-up and linearized. In this case, the water vapor molecules are not required to diffuse through the air/vapor mixture to reach the droplet surface. The rate of mass transfer to and from the droplet surface is controlled by kinetic theory of molecular collisions and the condensation rate is essentially instantaneous. The next step in complexity allows for a vapor/air mixture and the mass transfer ratio is now controlled by the diffusion rate of water vapor molecules through the mixture. This investigation process is allowing for carefully understanding the thermodynamic and acoustic processes of mass transfer that has already been developed in the literature.

Parallel to this work, sound propagation down a cylindrical tube was considered. Assumptions are that a layer of water (infinitely thin) always exists on the inner wall of the tube. The tube wall and water are rigid. Plane sound wave propagation in this media of gas/vapor mixture is considered and assumed to be an ideal gas. Like in the fog the vapor is allowed to condense (evaporate) to (from) the water layer. The same fundamental equations for the fog apply. There are four modes which are solutions to the linearized equations: acoustic, entropy and mass transfer modes and a vorticity mode. Each mode is a solution to the Helmholtz equation in cylindrical coordinates, for this geometry. The acoustic, entropy and mass transfer mode solutions are cylindrical Bessel functions with components in both radial and longitudinal directions. The vorticity mode solution is also a cylindrical Bessel function, but with cross coordinate terms.

The boundary conditions which were applied are the longitudinal velocity of the vapor at the wall is zero, the temperature at the wall is constant due to the high heat capacity of the wall. The vapor pressure at the wall depends only on the wall temperature, which means the mixture at the wall is pure vapor. The last boundary condition was that the gas cannot enter the tube wall, so the radial component of the vapor velocity is zero at the wall. Low- and high-frequency solutions for the longitudinal absorption coefficient shows less than a 1% increase in the absorption at 20° C compared to Zwikker and Kosten's[4] solution, which considers viscosity and heat conduction alone. In these assumptions a temperature gradient was not allowed to exist in the water layer. This gradient will allow for the latent heat produced by condensation to be conducted away.

In a third effect, a relatively simple extension of a previously made measurement was carried out in an attempt to detect the phenomenon of mass transfer. We have carried out specific acoustic impedance measurements in a dry and then wet, air-filled, model porous solid. This type of porous solid was previously studied and modeled in our laboratories.[5,6] We have improved on the technique previously used in that we can now separate changes in the specific acoustic impedance due to geometrical (wall porosity) effects and changes due to the presence of very small amounts of absorbed water. We have also extended the frequency range of the specific acoustic impedance measurements from 1.2 kHz up to 3.8 kHz.

We performed impedance measurements on a dry, porous wall sample. After these measurements were made, we closed off the pores in the ceramic walls by successively coating the walls with a very thin layer of polyurethane varnish diluted with one equal part of mineral spirits. We spooned the varnish into the pores and drained the excess varnish by shaking the sample at regular intervals in the first few hours after applying the varnish. We then dried the sample for at least 24 hours before making acoustic measurements at successive varnish layers. Data taken after 4 hours did not change but still final data was taken only after one day.

Measurements for real part of the specific impedance of the fifth, sixth, and seventh layers did not change to within ± 0.5% in frequency and ± 0.8% in amplitude. We interpret these results

to indicate that at the fifth varnish layer the walls have become nonporous, yielding a porous sample consisting of straight, square pore, flat wall capillaries.

To test the effect a thin film of water absorbed on the pore walls might have on the attenuation mechanisms in the porous sample, we then carried out measurements on the seven-layer varnished sample for two cases. After drying the sample at 110°C for one day, we mounted the sample and continuously made measurements as it cooled off. When the sample reached thermal equilibrium after several hours, the measured normalized impedance was within the experimental accuracy of the measurements done before oven drying the sample. We then wet the sample with a solution of water and Photo Flo 200. The Photo Flo is a surfactant. By weighing the sample dry and wet and calculating the available surface area we estimate a water film of thickness 7 μm. When the acoustic impedance was remeasured, the real part was reduced by 10%.

From the measured real and imaginary parts of the impedance and with use of the square pore model, one can solve numerically for the attenuation coefficient α and the phase speed c as a function of frequency. The results obtained from this numerical procedure are model dependent and, therefore, any definite conclusion as to the magnitude of the effect cannot be stated. But, barring this limitation, the results suggest an increased sound attenuation due to the presence of a thin water film.

Bass, Bauer and Evans[7] have measured the absorption coefficient of sound in air at 20° C as a function of relative humidity. To compare the magnitude of the absorption due to molecular thermal relaxation to the effect which we measure we take the maximum value of the absorption coefficient for our given frequency range as measured by Bass et al. We find that $\alpha \leq 10^{-3}$ dB/cm which is at most 100 times smaller than the observed effect we observed.

REFERENCES CITED

1. Michael Richardson, "Investigating the coastal benthic boundary layer," Eos, *Trans. Am. Geophys. Union,* **75(17)**, 21 and 205-206 (1994).

2. C.S. Cartens, "Quantifications of gas bubble and dissolved gas bubble and concentrations in organic-rich, muddy sediments," In *Coastal Benthic Boundary Layer Special Research Program: A Review of the First Year,* Vol. I, Michael Richardson (), pp. 119-124.

3. Nicholas P. Chotiros, "Reflection and reverberation in normal incidence echo-sounding," Submitted to *J. Acoust. Soc. Am.,* Fall 1994.

4. C. Zwikker and C.W. Kosten, *Sound Absorbing Materials* (Elsevier Publishing Co., Amsterdam, 1949).

5. Heui-Seol Roh, W. Patrick Arnott, James M. Sabatier, and Richard Raspet, "Measurement and calculation of acoustic propagation constants in arrays of small air-filled rectangular tubes," *J. Acoust. Soc. Am.,* **89**, 2617-2624 (1991).

6. W.P. Arnott, James M. Sabatier, and Richard Raspet, "Sound propagation in capillary tube-type porous media with small pores in the capillary walls," *J. Acoust. Soc. Am.*, **90(6)**, 3299-3306 (1991).

7. H.E. Bass, H.-J. Bauer, and L.B. Evans, "Atmospheric absorption of sound: analytical expressions," *J. Acoust. Soc. Am.*, **52**, 721 (1972).

AN ACTIVE RIGID WALL IMPEDANCE TUBE

ABSTRACT

The project brought about a completion to the Navy sponsored active surface research effort. The project addressed the Navy's need to have a fluid filled tube that would enable the determination of a material's acoustical properties. The intention was to advance the technology directly relevant to an active impedance tube. The research was also applicable to developing a method of measuring a fluid's homogeneous sound speed and attenuation. A paper submitted to the *Journal of the Acoustical Society of America* summarized results of this research.

INTRODUCTION

At low frequencies (below 2 kHz) the effects of fluid-wall coupling complicate the determination of a material's impedance when using a conventional "passive" impedance tube. A description of the active impedance tube prototype which was proposed to be built is given here. The active impedance tube has a cylindrical geometry with relatively thin walls to reduce discrepancies between the displacement of the tube's inner and outer radius. A plane wave sound source would terminate one end of the tube, and a material of unknown impedance would terminate the opposite end. A series of cylindrical piezoceramic rings would be placed in close contact with the outer diameter of the tube. Fifteen of the rings would be used to drive the wall of the tube. Another 15 of the rings would be used to detect $m = 0$ wall displacement. These rings would be evenly spaced along the axis of the tube, with sequential rings being alternatively used to drive the wall and to sense wall motion. First, the plane wave source and 15 piezoceramic ring drivers would be driven, one at a time, with a sinusoidal voltage. After collecting data from the 15 sensors for each case, a complex 15×15 matrix would be inverted to determine the proper gain and phase of the 16 independently driven channels (including the driving voltage of the plane wave source) to obtain zero output from each sensor while the plane wave source was being driven.

The materials needed to make such a tube were accumulated at the NCPA. For example, a digitally controlled system was constructed. The digital system was tested to insure its capability to simultaneously generate sinusoidal output on 16 independent channels, simultaneously receive input on another 16 independent channels and accumulate the complex Fourier amplitude of each input channel at the chosen frequency,. The digitizing rate for each of the 32 channels was 70 kHz.

After collaboration with Geoff Main at ONR it was determined that there was a need to focus on the basic research of how an active impedance tube might work, rather than working solely on the described experimental prototype. Experimental data was accumulated from an active impedance tube with a single input and output channel. This data clearly illustrated relevant technical issues to a larger scale version, and demonstrated agreement with theoretical equations used to model the combined effects of the piezoceramic ring, cylindrical tube, and fluid system.

The mathematical model developed for analyzing the active impedance tube demonstrated that difficult problems result from driving the tube wall in a discrete, rather than continuous manner. When a finite number of axial locations are given a radial stress, the radial displacement of the wall varies too quickly in between the drivers. Surprisingly, for a homogeneous elastic thin tube wall, the scale length of axial variations is about the same for all materials of the same thickness. The scale length of this axial variation varies as the square root of the tube's thickness. Making the tube thicker, however, increases the possibility of significant differences between the inner and outer tube radius, and this compromises the simplifying approach of only controlling the outer diameter of the tube.

Two solutions to this problem were proposed. One solution would be to design an active impedance tube that consists of a solid piezoceramic ring, without using a second type of tubing material underneath. Wrapping a resistive wire around the tube would axially interpolate applied voltages from a discrete number of output channels. A second approach would be to maintain the originally envisioned discrete driving scheme, but use a different criterion for controlling the wall other than driving the signals detected by an array of sensing piezoceramic rings to zero. By forming the tube into a torus, an external microphone could be used to determine when the average wall displacement between each of the driving rings went to zero. This would result in the wall being effectively rigid at wavelengths much longer than the spacing between drivers.

A different application can be considered for the case when there is no material of unknown impedance in a toroidal tube. The toroidal, wall driven, fluid filled tube should have a minimum in the external airborne sound field when driven at the frequency and wavenumber that excites plane waves within the fluid. In the torus, the wall is driven with a fixed wavelength and frequency is varied. The product of these two numbers gives the homogeneous fluid velocity when the external microphone detects a minimum. A future research effort could indicate the accuracy of this

method, and if the homogeneous attenuation of sound may be deduced from the amplitude of sound in the water at resonance, after accounting for attenuation due to the tube wall.

GRADUATE FELLOWSHIPS

The National Center for Physical Acoustics is an integral part of the University of Mississippi, which has a strong reputation for its graduate programs in physics, mathematics and engineering. Recruiting qualified US students into a Ph.D. program with research emphasis in acoustics is a high priority for NCPA. The NCPA fellowship program was developed with the hope that outstanding undergraduates would be identified and attracted to the University for specialized training in acoustics at NCPA. By offering these young scientists hands-on experience in this discipline, they would upon graduation be capable of filling positions in Navy Laboratories and/or facilities that conduct work relevant to acoustics.

In FY 91, NCPA received funds from the Office of Naval Research to administer a graduate fellowship program in acoustics. A limited number of applicants were awarded fellowships because of the high criteria we set for admission to this program and due to the limited number of available awards. The criteria for admission were revised further in 1993. We believe that this program has given more visibility to acoustics as a specialization in physics, and that visibility is in the best interests of the Navy. We wish to propose a continuation of this effort for FY 95.

Five NCPA Fellows were supported by these funds in the past year. These were:

Paul Elmore. Mr. Elmore's Ph.D. research involves studies of non–linearities in crystal structures. His research is directed by Dr. Mack Breazeale. Mr. Elmore successfully completed the comprehensive examinations in the fall of 1992 and expects to graduate in May, 1995.

John Kordomenos. Mr. Kordomenos came to us with an M.S. in high energy physics. He passed the comprehensive examinations early in the fall of 1993. He applied for an NCPA fellowship to begin in the fall of 1994 and was accepted. His research will be in thermoacoustics directed by Dr. Bass or sonoluminescence directed by Dr. Denardo.

Jay Lightfoot. As a freshman graduate student, Mr. Lightfoot performed extraordinarily well in freshman graduate courses in physics. His research in the area of thermoacoustics is directed by Dr. Bass. Mr. Lightfoot successfully completed the comprehensive exams in the fall of 1993. He expected to graduate in December, 1995.

Michael McPherson. Mr. McPherson was selected as an NCPA Fellow beginning in the fall of 1994. He is a graduate of Rhodes College in Memphis, TN.

Keith Olree. Mr. Olree has also proven to be an outstanding graduate student. He is doing research in active noise control under the direction of Dr. Shields. He also successfully completed the comprehensive exams in the fall of 1993. He expects to graduate in December, 1995.

The graduate fellowship program has proven to be one effective tool in recruiting outstanding students and provides these students an opportunity to perform innovative research.

During the past year, the NCPA Graduate Fellowship Selection Committee identified three outstanding students who met all qualifications. The first and third students on that list accepted. The limited number of qualified applicants is due in part to the stringent minimum qualifications (see Appendix III). It is our plan to reserve these fellowships for truly outstanding students only. In the future, special emphasis will be placed on recruitment of minorities and females. Each year, descriptive material is sent to historically black colleges and directed to personnel in their physics department.

NEW INITIATIVES IN THE PHYSICS OF ACOUSTICS

RESEARCH PROGRESS IN FY94

Several areas were considered for new thrusts in FY94. These included very short wavelength/high frequency acoustics (solid state), a program to allow Postdoctoral Research Associates funded time to pursue new research interests, physics of electrical discharges in water, nonlinear properties of solids, and buried object detection. We interviewed several possible scientists to work in one of these areas and finally chose to pursue buried object detection as the new initiative for FY94.

The choice of buried object detection as the new initiative for FY94 was based upon three factors. First, since establishing several years ago the physics associated with acoustic/seismic coupling as a means of imaging a buried mine,[1-3] personnel in this laboratory have discussed unresolved issues. We felt it was time to answer remaining questions and move on toward applications. Second, we have personnel in house to direct this effort so no long term commitments are required. The basic physics part of this research program can be completed in two years allowing an early decision about long term research prospects. Third, the candidate we were most impressed with to do the very high frequency work will require a tenure track position. At this point in time, we have not been able to extract such a commitment from the University although our request is being considered for FY 96 funding. This research project will allow us to treat some good physics in a short period of time while keeping our options open for future research initiatives.

The phenomenon of acoustic to seismic coupling is reasonably well understood, at least for frequencies up to 500 Hz and incident plane waves. The current state of understanding suggests that this effect might allow imaging of objects below a surface. Specifically, we are interested in

exploring the physics involved in imaging objects buried a few inches in soil and evaluating the feasibility of using this effect to design a system. Research began in September 1994 and we report progress to date.

Initially, we wanted to increase the bandwidth over which previous buried object measurements had been taken. The ratio of the normal surface velocity of the ground surface to the incident acoustic pressure is measured using a co-located geophone and microphone. An acoustic source broadcasting noise (1 – 3 kHz) is used to excite the ground surface. This measurement is termed the seismic/acoustic ratio (S/A).

In Figs. 1 and 2, the measured S/A ratio at a number of locations in the vicinity of a 4 inch and 2 inch diameter aluminum dish are shown. The dishes were 2 cm below the surface in dry sand. Contours represent constants for the integrated S/A ratio between 1 and 3 kHz. These data show a detection resolution of less than five centimeters (2 inches).

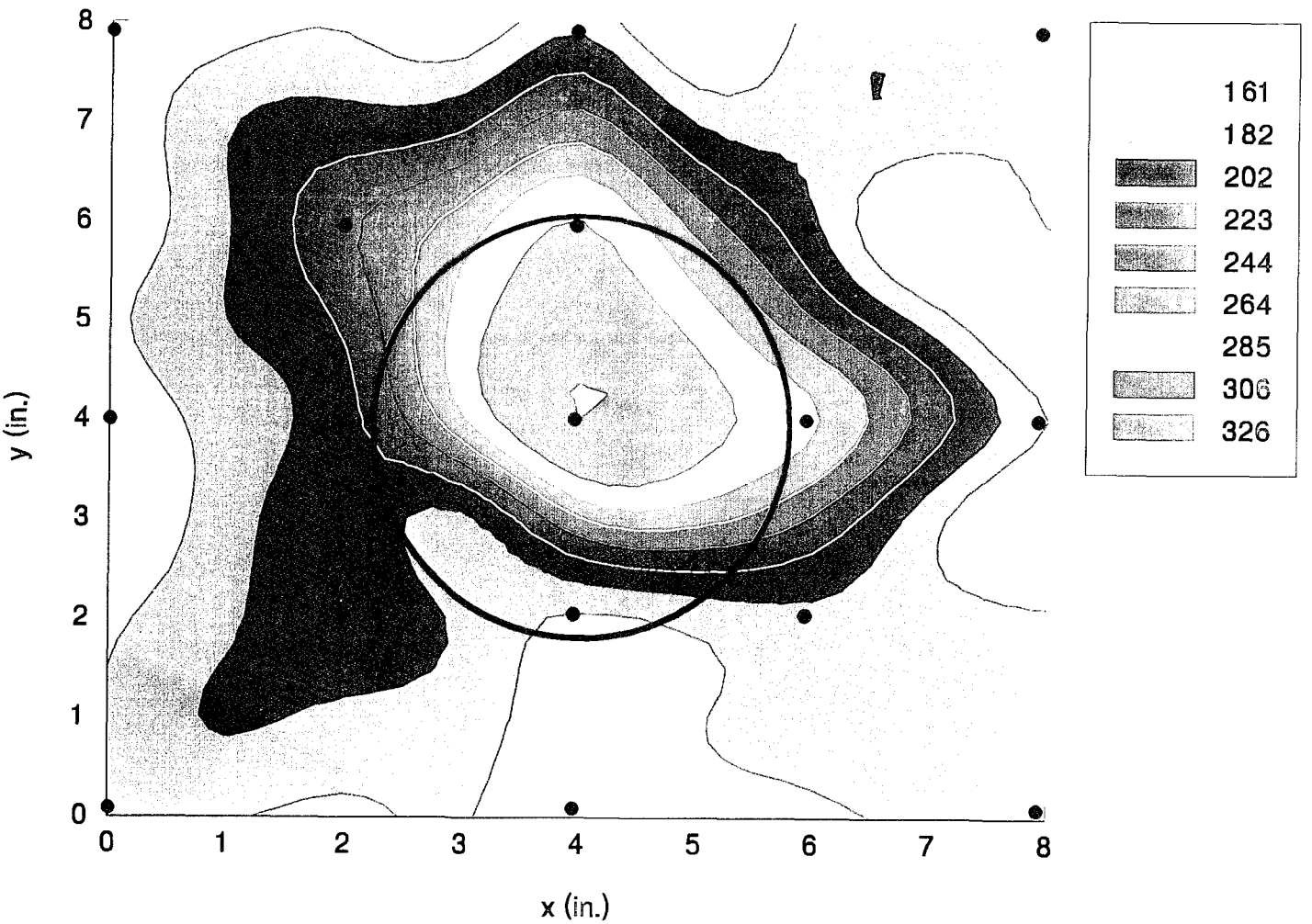

Figure 1. A contour map of constant S/A ratio for a 4-inch circular plate. The ● represents measurement locations. The position of the plate is shown by the solid circle.

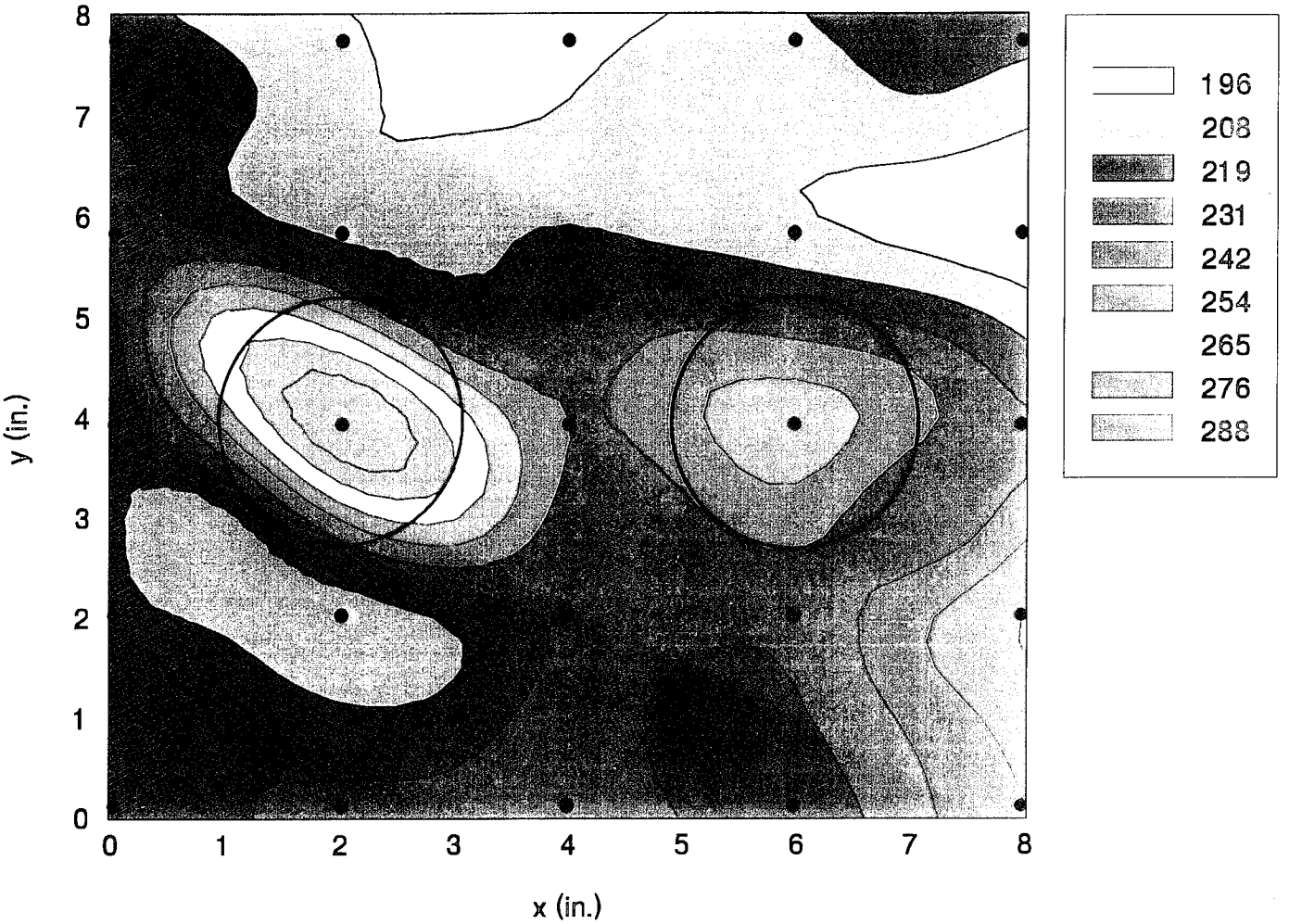

Figure 2. A contour map of constant S/A ratio for two 2-inch circular plates. The ● represents measurement locations. The positions of each plate are shown by the solid circles.